Influence of Pore Dimension and Sorption Configuration on the Heat of Sorption of Hexane on Monodimensional Siliceous Zeolites

Evgueni N. Gribov, German Sastre, and Avelino Corma*

Instituto de Tecnologia Quimica UPV-CSIC, Universidad Politécnica de Valencia, Av. Los Naranjos s/n, 46022 Valencia, Spain

Received: May 11, 2005; In Final Form: October 17, 2005

Sorption of *n*-hexane on monodimensional pure silica SSZ-35, CIT-5, ZSM-12, and ZSM-22 zeolites with different pore dimension and on recently synthesized ITQ-29 was studied by IR spectroscopic and computational chemistry methods. Heats of sorption of *n*-hexane on these zeolites was determined experimentally from the temperature dependence of the intensity of IR bands of sorbed hexane as well as from theoretical calculations. Calculations have shown the different orientations of sorbed hexane molecules inside zeolite channels, which depend on the type of zeolite and loading. At high loadings, ordering of hexane inside the channels is observed due to optimization of sorbate−sorbate and sorbate−zeolite interaction energies. Such ordering is responsible for the increase of the sorption energy. A decrease of the sorption energy upon increasing the pore dimension of zeolite was observed, in agreement with results previously published in the literature. Effects of pore diameter of zeolites and ordering of molecules inside zeolite channels on the sorption energy of hexane are discussed.

Introduction

Zeolites are widely used as solid-acid catalysts in many industrial processes like cracking, skeletal isomerization, alkylation of hydrocarbons, synthesis of alcohols, ketones, and other important organics.[1−3] For a given catalytic reaction the activity of zeolites is characterized by the extent of decrease of the activation barrier between the sorbed reagent and the activation complex. This barrier is characterized by the apparent activation energy, which could be written as the sum of the real activation energy and sorption enthalpy ("sorption effect"[4]).

$$E_a^{app} = E_a^{real} + \Delta H_{ads}$$

From this equation it is clear that the heat of sorption plays an essential role in the catalytic performance of zeolites, decreasing the activation barrier of the reaction, and from this point of view the study of the sorption properties of hydrocarbons on different solids and especially on zeolites becomes very important. A large number of works related to this topic and performed by different experimental (FTIR, volumetry, NMR, chromatography, calorimetry) and theoretical methods have been published.[5−35] From a literature review it can be concluded that the heat of sorption depends on parameters such as the properties of the probe molecule, the type of zeolite, its channel structure (dimension and tortuosity),[19,22,25,36] chemical composition (Si/Al ratio), and the presence in the framework of atoms other than Al.[19,31]

As far as the nature of the hydrocarbon is concerned, a linear increase of the sorption enthalpy when increasing the alkane carbon number (usually of ∼9 to ∼15 kJ/mol per added $-CH_2-$ group[37,38]) was observed and explained by the additive character of the dispersive forces involved.[12,15,22,31] The correlations of the heat of sorption of different probe molecules with their physical and structural parameters (the critical parameters of gases, proton affinity, polarizabilities) were also studied,[39−41] but valid correlations for all types of probe molecules are still not available.

Regarding the effect of zeolite parameters on the heat of sorption, it has been proposed that the energy of sorption is markedly influenced by the fit between the pore dimension of zeolite and the size of the molecule sorbed.[16,17] Such a correlation suggests that an optimum situation between the hydrocarbons and the zeolite structure should exist and that this fit should depend on the shape of the molecule.[19] In fact, the optimum sorption energy of *n*-alkanes in all-silica zeolites is claimed for zeolites with an average pore diameter between 4 and 5 Å,[8] which is very close to the kinetic diameter of hexane (4.3 Å[7]).

For zeolites with larger pore dimension (more than the optimal 4−5 Å) the heat of sorption should be lower due to lower interaction of the molecules with the walls of the zeolite. Such a phenomenon was observed upon sorption of *n*-paraffins on microporous as well as on macroporous (up to 10 nm[42]) zeolites and zeotypes, i.e., hexane on siliceous MCM-41 by volumetry,[36] hexane and benzene on aluminophosphates with the 4−12 Å pore dimension range,[25] or acidic zeolites (FER, TON, MFI, MOR, FAU, and KFI) with different dimensionality.[19]

It has also been claimed that when the zeolite pore diameter is lower than 4−5 Å, the sorption energy should decrease owing to the higher repulsion forces between sorbed molecules which begin to play a considerable role at pore size smaller than 0.5 nm.[19] The effects derived from the close fitting of probe molecules with the dimension of zeolite channels were first considered by Derouane and associated with a "nest effect".[17] This effect was used to explain the increase of the sorption heat upon decreasing the pore diameter of zeolites by an electronic "confinement effect".[43,44]

Besides correlating the heat of sorption with pore dimension, as was first suggested by Barrer,[45] this has also been correlated

* Corresponding author: Ph +34-96-387-7800; Fax +34-96-398-7809; e-mail acorma@itq.upv.es.

10.1021/jp052462a CCC: $30.25
Published on Web 11/30/2005

TABLE 1: Literature Data of Sorption Heat of Hexane on Different Zeolites and Aluminophosphates

IZA code[71]	heat, kJ/mol (method[a]; **Si/Al ratio**[b])[ref]
AEL	74.5 (cal; **AlPO**)[32,78]; 79 (sim; **AlPO**)[25]; 81.2(TG; **AlPO**)[25]; 65.5 (TG-cal; **AlPO**)[16]; 76.5−78[c] (cal; **AlPO**)[46]; 70.6 (sim; **sil**)[80]
AET	42.9 (sim; **sil**)[34]
AFI	59.0−60[c] (cal; **AlPO**)[32,46,78]; 68.8 (TG; **AlPO**)[25]; 53.4 (sim; **AlPO**)[23]; 67 (sim; **AlPO**)[25]; 54.6 (TG-cal; **AlPO**)[16]; 56.5 (g; **AlPO**)[27]; 57.4 (sim; **AlPO**)[77]; 68.4 (TG; **sil**)[25]; 54.1 (chr; **sil**)[14]; 67 (sim; **sil**)[25]; 54.0 (sim; **sil**)[34]; ∼57−60[c,d](cal; **58**)[65]
AFR	46.5 (sim; **sil**)[34]
ATO	77.4 (TG; **AlPO**)[25]
BEA	55.1 (sim; **sil**)[34]; 63.4 (chr; **150**)[7]; 71 (kin; **14**)[67]; 62.7 (chr; **12**)[15]
CFI	55.8 (sim; **sil**)[34]
CON	57.6 (sim; **sil**)[34]; ∼63−65[c,d] (cal; **21**)[65]
DON	∼49.3[e] (sim; **sil**)[26]; ∼45.0[e] (cal; **sil**)[6]; 44.4 (sim; **sil**)[34]
EMT	53 (g, cal; **3.8**)[20]
FAU	47.3−55[c] (cal; **sil**)[32,46,78]; 33.1 (sim; **sil**)[34]; 37.5 (sim; **sil**)[8]; ∼49.4[e] (cal; **sil**)[6]; 53 (g, cal; **300**)[20]; 60 (TPD-TG; **17**)[24]; 53 (g, cal; **2.7**)[22]; 49.28 (chr; **13X**)[81]
FER	∼77.8[e] (sim; **sil**)[26]; 77.6 (sim; **sil**)[8]; 87.2 (TG, cal)[16]; 79 (g, cal; **30**)[19]; ∼92.1[e] (cal; **22**)[6]
GME	49.0 (sim; **sil**)[34]
LTA	41.2 (sim; **sil**)[8]; 29.84 (chr; **3A**)[69]; 27.467 (chr; **3A**)[9]; 42.5 (chr; **4A**)[69]; 59.6 (g; **5A**)[82]; 27.54 (chr; **5A**)[69]; 34.723 (chr; **5A**)[9]; 57.97 (chr; **5A**)[81]
LTL	41.8 (sim; **sil**)[34]
MAZ	49.6 (sim; **sil**)[34]
MEI	45.9 (sim; **sil**)[34]
MEL	74.5−82[c] (cal; **sil**)[46]; ∼78−80[c,d] (cal; **23**)[65]
MFI	∼60−100 (see references)[31,83]
MOR	58.8 (sim; **sil**)[34]; 59.0 (cal; **140**)[32,46]: ∼65−67[c,d] (cal; **79.4**)[65]; 69 (kin; **10**−**35**)[67]; 69 (g, cal; **10**)[22]; 68.0 (TG, cal; **9**)[16]; 67.1 (chr; **5**)[15]
MTT	67.1 (sim; **sil**)[80]
MTW	∼68.9[e] (sim; **sil**)[26]; 69.3 (sim; **sil**)[34]; ∼62.7[e] (cal; **140**)[6]; ∼70−77[c,d] (cal; **97**)[65]
MWW	54 (sim; **sil**)[84]; 46.9 (TG; **sil**)[85]; 69[86]
OFF	56.1 (sim; **sil**)[34]
RHO	43.3−46.1 (sim; **sil**)[8]
SFE	59.9 (sim; **sil**)[34]
TON	74.5 (sim; **sil**)[80]; ∼73.7[e] (sim; **sil**)[26]; ∼81.5[e] (cal; **52**)[6]; 81.5 (g, cal; **45**)[19]; 82 (kin; **39**)[67]; 75.0 (chr; **30**)[15]; 77.1 (chr; **30**)[79]
VET	66.2 (sim; **sil**)[34]
VFI	42.5−50[c] (cal; **AlPO**)[32,46,78]; 35.4 (sim; **AlPO**)[77]; 50 (sim; **AlPO**)[25]; 48.1 (TG; **AlPO**)[25]
others	SSZ-31: 61.1 (sim; **sil**)[34]; KFI: 60 (g, cal; **4**)[19]; IM-5: 77−80[c,d] (cal; **16**)[87]; MCM-41: 63−78 (vol; **sil**)[88], 32−39 (vol; **sil**)[36]; Mg-saponite: 34 (kin; **5.5**)[67]; SiO_2: 30 (chr)[68]; carbon: 55.43 (chr)[81], 61−72 (TG, cal)[89], 35.1−46.9 (chr)[90]; alumina: 31.81 (chr)[81], 41.012 (chr)[9]; methylsilicon: 28.4 (chr)[91]; polydimethylsilicon: 24 (chr)[68]

[a] cal = calorimetry, TG = thermogravimetry, sim = simulations, chr = chromatography, g = gravimetry, TPD = thermoprogrammed desorption, kin = kinetic, and vol = volumetry. [b] sil = siliceous, AlPO = aluminophosphates, 3A, 4A, 5A, 13X = names of zeolites, and numbers correspond to a Si/Al ratio. [c] Depending on the loading. [d] Estimated from the graph. [e] Values estimated for *n*-hexane from the reference papers on the basis of the linear dependence of the heat of sorption on the carbon number.

with the framework density of zeolites;[19,32,46] in this case zeolites with different dimensionality could be compared. It has been shown that the heat of sorption usually increases upon increasing the framework density,[19,32,46] indicating a higher strength of interaction between the zeolite lattice and the sorbed alkane.[19] In a better generalization, a linear correlation between the heat of sorption and the electronegativity of framework oxygen atoms in zeolites, aluminophosphates, and other solids (which is in turn correlated with the framework density) was suggested.[46]

In this work we have carried out a systematic theoretical and experimental study of the adsorption of *n*-hexane on a series of pure silica monodimensional zeolites with different pore diameters. The heats of sorption of hexane have been determined while considering the orientation of the molecules inside the channels at different loadings. The results have been rationalized and compared, when available, with those reported in the literature (see Table 1).

Experimental Details

Materials. In this work pure silica zeolites were synthesized according to the following references: ITQ-29,[47] SSZ-35,[48] ZSM-22,[49] CIT-5,[50] ZSM-12.[51] All zeolites were studied by XRD, which showed good crystallinity of the structures. The details of the XRD studies can be found in refs 47, 48, 50, and 51.

IR Adsorption. The experiments were performed with a FTIR spectrometer FTS-40A Bio-Rad in the transmission absorption mode. The zeolites were pressed to a self-supporting wafer and introduced into the heatable sample holder of a vacuum cell. The samples were activated by heating at 500 °C in a vacuum for 2 h and cooled to adsorption temperature. The experiment of adsorption of hexane was performed in the 100−200 °C temperature interval and in the pressure range from 1 to 50 mbar. In all experiments the gas-phase spectrum of hexane recorded at the same temperature and pressure as well as sample background spectrum was subtracted. The uptake of hexane was calculated in arbitrary units from the integral intensities of the absorption bands in the 2800−3100 cm^{-1} region due to the stretching vibrations of the CH_2 and CH_3 groups, according to ref 52.

The heat of sorption on zeolites was calculated using the Langmuir approach (1).[53]

$$\theta = \frac{K_s P}{1 + K_s P} \tag{1}$$

Equation 1 can be transformed into eq 2 by considering $\theta = A/A_{max}$

$$A = \frac{A_{max} K_s P}{1 + K_s P} \quad (2)$$

where K_s is the sorption constant, P is the pressure, A is the integral intensity of the given IR band, and A_{max} is the integral intensity of the same band at the maximum loading.

Equation 2 can be written in reciprocal coordinates as

$$\frac{1}{A} = \frac{1}{A_{max}} + \frac{1}{A_{max} K_s P}$$

From the angular coefficient of the linear dependence of the $1/A$ on the $1/P$, the sorption constant (K_s) can be determined at any given temperature. From the Clausius−Clapeyron relation of $\ln(K_s)$ vs $1/T$, the heats of sorption were determined for different zeolites. For application of the Langmuir equation we have considered that the sorbate−sorbate interactions are much weaker than the sorbent−sorbate interactions taking into account the work of Richards and Rees.[54] Furthermore, the Langmuir model has been applied successfully before for adsorption isotherms on pure silica ITQ-1.[55] In agreement with the above, we have seen that the Langmuir model also fits very well our experimental results on pure silica zeolites.

Computational Methods

The calculations have been performed using lattice energy minimization techniques[56] and the GULP code,[57] employing the Ewald method for summation of the long-range Coulombic interactions, and direct summation of the short-range interactions with a cutoff distance of 12 Å. The RFO (rational function optimization) technique was used as the cell minimization scheme with a convergence criterion of a gradient norm below 0.001 eV/Å. The empirical shell model force field for zeolites[58,59] has been used throughout. For the calculations including the effect of the hexane molecules, the force fields by Kiselev et al.[60] and by Oie et al.[61] have been used for the hexane−zeolite and hexane−hexane interactions, respectively. For hexane, the Mulliken charge distribution has been obtained by means of the quantum chemistry Hartree−Fock method by using a 6-31G**[62] basis set, and the calculations have been performed by means of the NWCHEM package.[63] The total potential energy function and the respective terms are as follows:

$$E_{zeo'} = E_{Buckingham} + E_{Coulombic} + E_{three-body} + E_{core-shell} \quad (3)$$

$$E_{hexane} = E_{two-body} + E_{three-body} + E_{four-body} + E_{Coulombic} \quad (4)$$

$$E_{zeo'-hexane} = E_{Lennard-Jones} \quad (5)$$

The computational total energy minimizations take into account that the stabilization of the "zeolite−hexane" system with respect to the separate components is due to several energetic interactions between the guest and the zeolite as follows:

$$E_{total} = E_{zeo'} + E_{zeo'-hexane} + \Delta E_{hexane} \quad (6)$$

The first term, $E_{zeo'}$, refers to the stability of the final zeolite formed, which is formed with hexane occluded. More stable structures will have less energy and therefore will be favored. Note that we have indicated zeo′ to refer that the final optimized structure differs from an optimization without hexane molecules occluded. Therefore, the flexibility of the structure and not only its intrinsic stability will contribute to this term, although it is expected that the latter will be the most important contribution.

The contribution $E_{zeo'-hexane}$ corresponds to the interactions between the zeolite structure and the hexane molecules, and this is what we relate to the calculated heat of sorption. This term is more favorable when an adequate match between the hexane shape (which is allowed to fully relax during the energy minimization) and the micropore is observed. Given the apolar character of the paraffinic hydrocarbon, the most important contribution to this term will be the short-range interactions which account mainly for the electronic interactions between the organic and the zeolite walls. Nevertheless, the hexane atomic charges and the zeolite charges have also been taken into account in the calculation.

The other term is ΔE_{hexane}, which amounts for the hexane deformation as occluded in the zeolite micropore. To analyze the final optimization results with chemical sense, the hexane sorption process should not impose too restrictive conformations of hexane within the zeolite micropores. Therefore, we have checked the amount of this term, ensuring that in all cases its contribution is negligible, and therefore the hexane molecules are adsorbed without imposing high-energy conformations. In fact, in all cases, less than 2 kJ/mol is obtained for the hexane deformation energy.

Results

Sorption of Hexane on Zeolites. In this work we have studied monodimensional siliceous zeolites with different pore size. Isotherms of hexane on CIT-5 (A), SSZ-35 (B), ZSM-12 (C), and ITQ-29 (D) are well fitted by the Langmuir equation, as can be seen in Figure 1. The angular coefficient of $\ln(K_s)$ plotted against $1/T$ (Arrhenius coordinates) gives us the enthalpy of sorption. The results are present in Figure 2. In Table 2, the heats of sorption of hexane determined experimentally by IR spectroscopy and calculated theoretically are shown and compared with those reported in the literature. As can be seen, a fair agreement exists with Table 2; generally, relatively good agreements with the literature data are observed.

SSZ-35 (STF Structure). This zeolite has a complex unidimensional pore system consisted of stacked cages (ABC stacking) with repeated 10 MR (5.5 × 6.1 Å) and 18 MR (12.5 × 9 Å) windows aperture. The average pore diameter of 10 MR is 5.65 Å.[48] Theoretical calculations show that the configurations of molecules sorbed in the channels of SSZ-35 zeolite and, hence, their sorption properties depend on loading. At low loading hexane molecules are located between the 18 MR and 10 MR rings (see Figure 3), mainly parallel to the channels. The center of mass of the hexane molecule is centered exactly in the 10 MR and slightly moved from the center of the channels. At higher loading (1 molecule/16 SiO_2 units) hexane is ordered inside the channels in such a way that an angle of ∼45° is formed between the channel direction and the hexane molecule axis (see Figure 4a). In this structure $-CH_3$ groups located at both ends of the hexane molecule are interacting with the two nearest 10 MR windows. This situation is shown in detail in Figure 4b. Such ordering contributes to the increase of the sorption energy from 54.4 kJ/mol (at low loading) to 62.3 kJ/mol (at higher loading). The sorption energy obtained by FTIR spectroscopy (57 kJ/mol) is within this theoretical interval (see Table 2). Because of the lack of the literature data, the heat of sorption of hexane on the SSZ-35 zeolite can be compared only with that found in the literature for other monodimensional zeolites with similar pore diameter. Values of 56.1 kJ/mol[34] and 54−60 kJ/mol[34,64] have been obtained for *n*-hexane sorbed on OFF (12 MR channels with 6.7 × 6.8 Å pore aperture) and for AFI (12 MR channels with

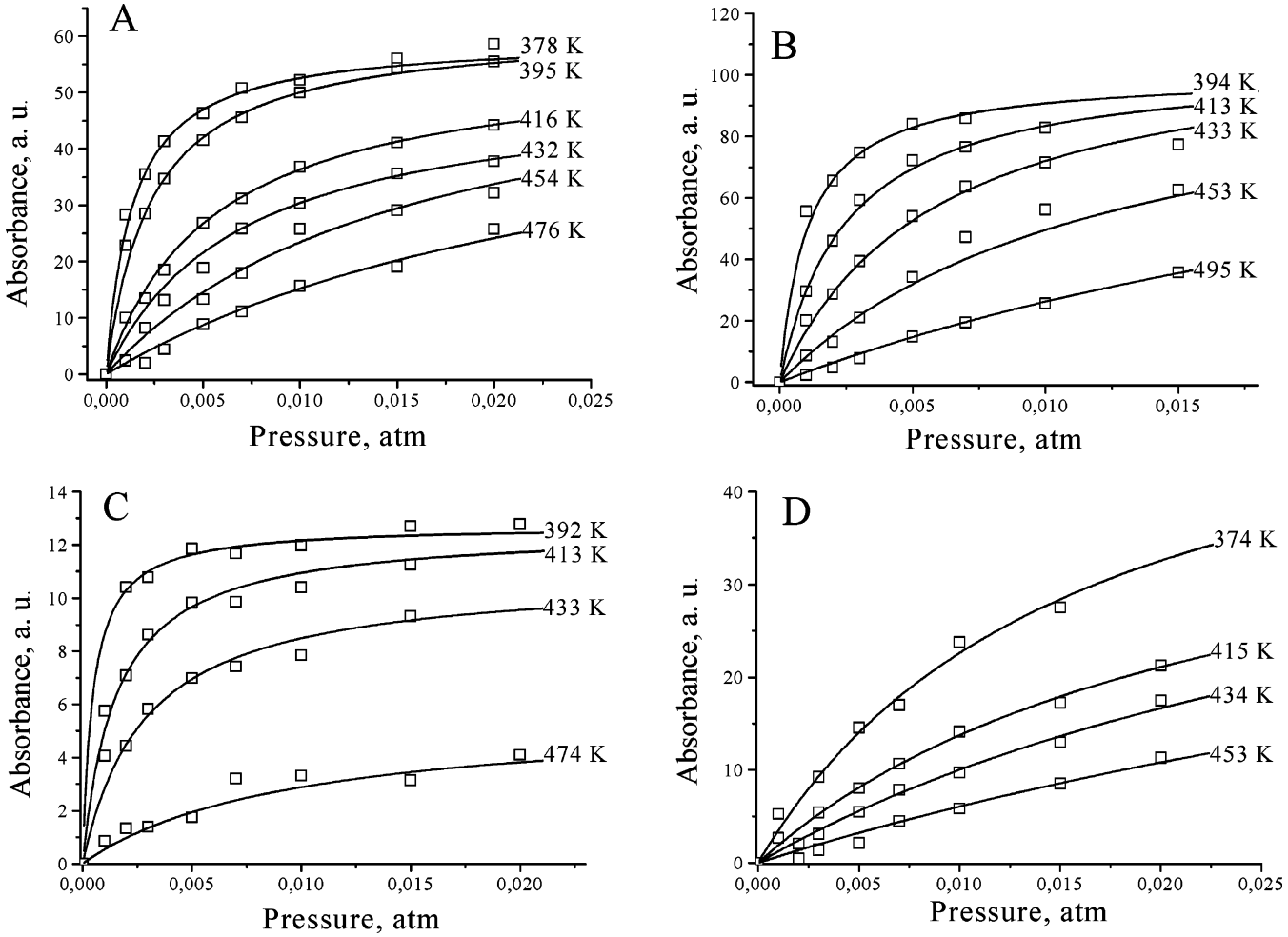

Figure 1. Sorption isotherms obtained by IR spectroscopic method of hexane sorbed in the 120−220 °C temperature interval on siliceous zeolites: (A) CIT-5, (B) SSZ-35, (C) ZSM-12, and (D) ITQ-29. For each isotherm temperature is shown on the right part. Experimental plots were fitted by the Langmuir equation.

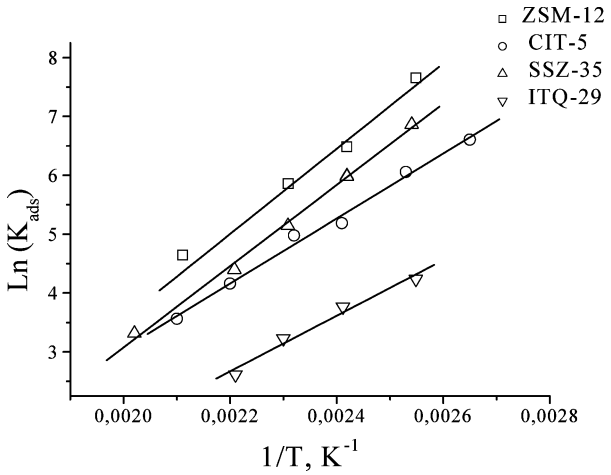

Figure 2. Arrhenius plots of ln(K_s) plotted vs 1/T, obtained for CIT-5, SSZ-35, ZSM-12, and ITQ-29 siliceous zeolites.

7.3 × 7.3 Å pore diameter), respectively. Taking into account the above results, we can say that although the pore structure of SSZ-35 zeolite can be described as intermediate between 18 MR and 10 MR, from the point of view of the heat of sorption, SSZ-35 is close to 12 MR zeolites.

ZSM-12 (MTW Structure). This zeolite consists of 1-dimensional channels with 12-membered rings with diameter of 6.0 × 5.6 Å. Theoretical calculations showed that also for this zeolite sorption properties depend on the loading. At low loading (1 molecule/42 SiO_2 units) hexane is sorbed mainly parallel to the channel direction and slightly moved from the centers. A small fraction of molecules exists where the molecules are centered strictly in the channels and slightly inclined. This situation is shown in Figure 5. At high loading (1 molecule/14 SiO_2 units) molecules are ordered inside the pores with an angle of about 45° between the channel direction and the axis of the hexane molecule (Figure 6).

The theoretically calculated heat of sorption was found to increase from 64.2 kJ/mol at low loading to 70.2 kJ/mol at high loading, the last value being very close to the one we obtained experimentally (72 kJ/mol). These values are in agreement with the literature data, which are range from 69.3 kJ/mol[34] to 77 kJ/mol,[65] variations being probably due to differences in sample quality and loadings.

CIT-5 (CFI Structure). This zeolite has unidirectional 14 MR channels with a diameter of 7.3 Å.[50] From the Ar isotherm the mean microporous diameter was estimated to be 6.4 Å.[50,66] From theoretical calculations we found that at high loading (1 molecule/16 SiO_2 units) hexane is ordered inside the 14 MR channels perpendicularly to the zeolite wall as is shown in Figure 7, the distance between sorbed hexane molecules being ∼4 Å. For low loadings no calculations were done.

The heat of sorption obtained theoretically was 55.6 kJ/mol, which is in excellent agreement with the literature data 55.8 kJ/mol.[34] Experimentally determined sorption heat was found to be lower (46 kJ/mol) than the data mentioned before and

TABLE 2: Heats of Hexane Sorption Obtained in This Work and Compared to the Literature Data

zeolite	IZA code[71]	structure, pore dimension, Å	heats of sorption, kJ/mol		
			from IR	from calculations	from literature
SSZ-35	STF[a]	**10**, 5.5 × 6.1 **18**, 12.5 × 9	57	62.3 ± 1.5[b] 54.4 ± 2.6[c]	
ZSM-12	MTW	**12**, 5.6 × 6.0	72	70.2 ± 0.1[b] 64.2 ± 2.5[c]	70−77;[65] 69.3[34]
CIT-5	CFI	**14**, 7.3 × 7.55	46	55.6 ± 0.4	55.8[34]
ZSM-22[d]	TON	**10**, 4.6 × 5.7	83	75.7 ± 0.4	75;[15] 82;[67] 77.1;[6]
ITQ-29	LTA	supercages 11.4 Å	39	52.3 ± 2.7[e] 54.1 ± 1.1[f] 46.6[g]	41.2[8]
SSZ-24	AFI	**12**, 7.3 × 7.3		56.9 ± 1.1	54−68[25,14]

[a] Explanation of STF structure is in the text. [b] High loading. [c] Low loading. [d] This zeolite has ratio Si/Al = 50, but hexane is sorbed mainly inside the pores and not on Brønsted sites, as was seen from the IR spectra. [e] 3 hexanes per supercage. [f] 2 hexanes per supercage. [g] 1 hexanes per supercage.

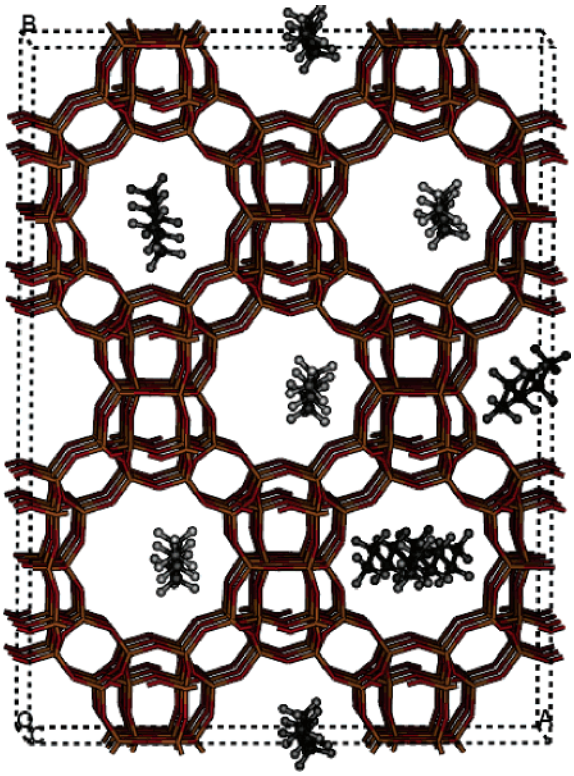

Figure 3. Optimized hexane molecules in SSZ-35 zeolite. This corresponds to a loading of 1 hexane/48 SiO_2 units.

can be compared to the heat of hexane sorption on DON, ≈49 and ≈45 kJ/mol (data taken from the ref 26 and 6, respectively, and interpolated to hexane on the basis of the linear dependence of the sorption heat on the number of carbon atoms), which has larger pores (8.1 × 8.2 Å) than CFI structure (7.2 × 7.5 Å). The theoretical heat of sorption found in our work is very similar to that calculated for hexane on AFI-type structure, 56.9 kJ/mol. AFI structure represents monodimensional pore channels with 12 MR having a diameter of 7.3 × 7.3 Å.

ZSM-22 (TON Structure). This zeolite has monodimensional channels with 10 MR of 5.7 × 4.6 Å diameter. Because of the lowest pore aperture of the channels, which is very near to the kinetic diameter of hexane molecule, 4.3 Å,[7] we expect that due to the "confinement effect" it will have the highest heat of sorption. In fact, the sorption energy of 83 kJ/mol experimentally obtained, which is in agreement with the literature data: 75,[15] 82,[67] and 77.1 kJ/mol[6] are the highest we have found for different zeolites studied. The location of hexane molecules inside the zeolite channels at loading of 1 molecule/

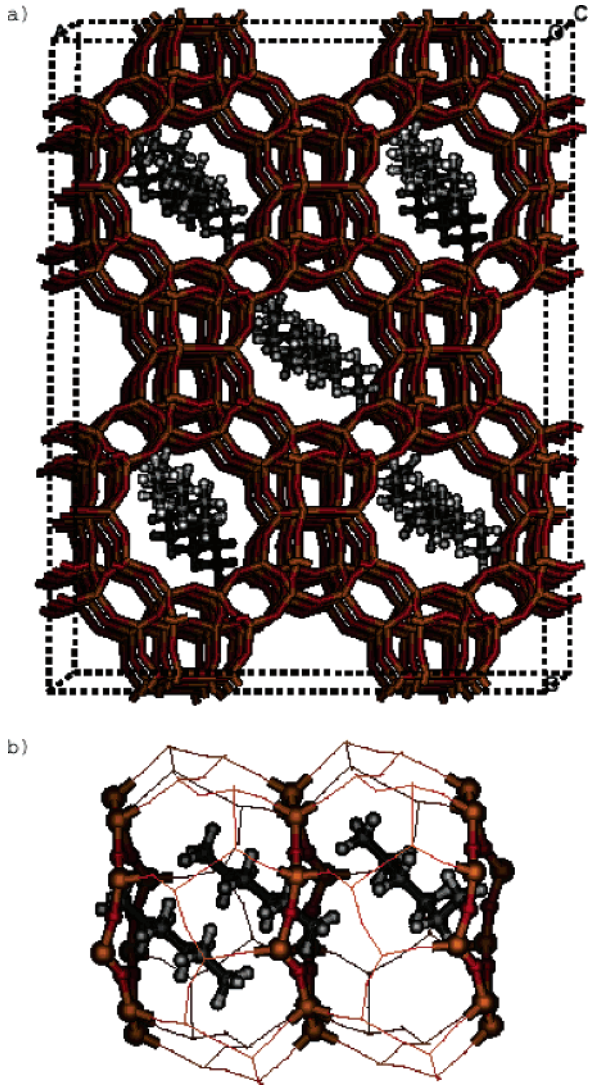

Figure 4. (a) Optimized hexane molecules in SSZ-35 zeolite. This corresponds to a loading of 1 hexane/16 SiO_2 units. (b) Details of optimized hexane molecules in the cavity of the SSZ-35 zeolite.

36 SiO_2 units is shown in Figure 8. As is seen there, hexane is sorbed in the center of pores parallel to the channel direction. The heat of sorption calculated is 75.7 kJ/mol, which is lower than that obtained by IR (Table 2).

ITQ-29 (LTA Structure). The structure of LTA consists of the sodalite cages with average diameter of 6.6 Å connected by double four-member rings and forming supercages with 11.4 Å diameters. Sodalite cages are accessible from the supercages

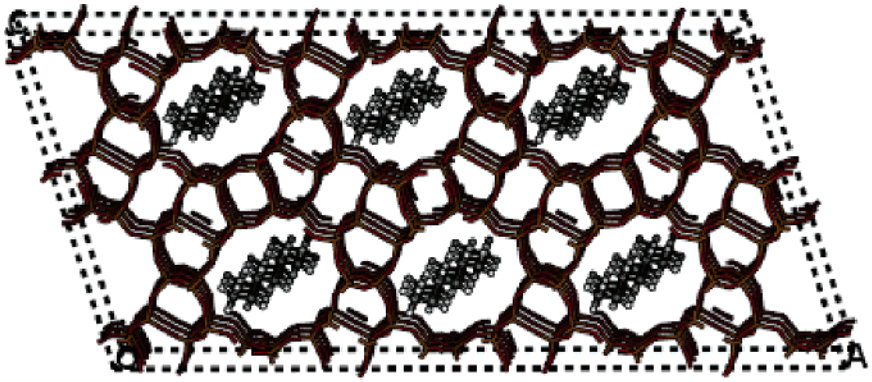

Figure 5. Optimized hexane molecules in ZSM-12 zeolite. This corresponds to a loading of 1 hexane/42 SiO_2 units.

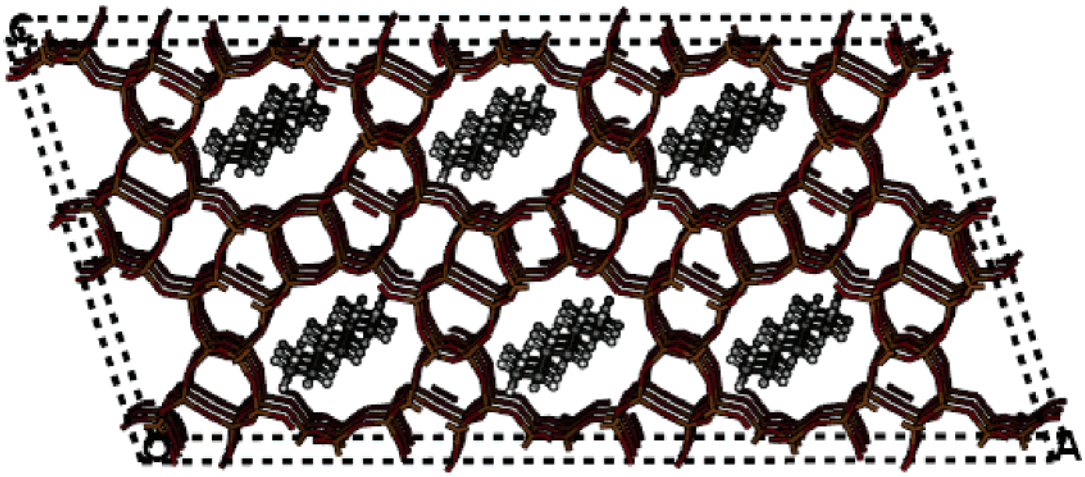

Figure 6. Optimized hexane molecules in ZSM-12 zeolite. This corresponds to a loading of 1 hexane/14 SiO_2 units.

by 6 MR windows, which are too small to allow the hexane molecule to penetrate into sodalites. Thus, we expect that hexane will be sorbed only inside super cages with low interaction energy, and the sorption properties relevant to this work should be somehow similar to hexane in a FAU zeolite. In fact, a sorption energy of 39 kJ/mol was found from FTIR spectroscopy, which should be compared to the heat of sorption of hexane calculated on LTA (41 kJ/mol[8]) zeolites and the values experimentally obtained on amorphous silica (30 kJ/mol[68]), 3A (27−30 kJ/mol[9,69]), 4A (42.5 kJ/mol[69]), and 5A zeolites (27.5,[69] 34.7 kJ/mol[9]). It should be noted that our value is very similar to that reported for hexane sorbed on a siliceous MCM-41 mesoporous molecular sieve (32−39 kJ/mol for the 31−99 Å pore range[36]). A similar interaction energy found for ITQ-29 and MCM-41 means that the electrical field inside the large supercages of ITQ-29 zeolite (11.4 Å) does not affect much the sorption properties of *n*-hexane. This is in agreement with the statement that in all-silica small pore zeolite the electric field does not vary much across the channel, and as a consequence the Coulombic term can often be neglected.[70]

Theoretically calculated heats are larger and very little dependent on the loading: 52.3 kJ/mol (3 molecules in supercage), 54.1 kJ/mol (2 molecules in supercage), and 46.6 kJ/mol (1 molecule in supercage) (see Table 2). Optimized configurations of hexane sorbed in ITQ-29 are shown in Figure 9 (3 molecules in supercage). For a loading of 1 molecule per supercage, both $-CH_3$ ends of hexane are interacting with the 8 MR, which explains the relatively high calculated interaction energy (46.6 kJ/mol) compared to that reported in the literature (41 kJ/mol[8]). Upon increasing the loading the energy increases to 54.1 kJ/mol (for 2 molecules in supercage) and to 52.3 kJ/mol (for 3 molecules per supercage), while the sorption structure of hexanes is not changed. The high heat of sorption demonstrates a very good fitting of hexane inside supercage of ITQ-29 zeolite. The difference of experimentally obtained sorption energy (39 kJ/mol) and theoretically calculated could be (46.6−52.3 kJ/mol) due to a higher loading in the former case, when adsorption of hexane occurs on the external surface.

SSZ-24 (AFI Structure). This zeolite has monodimensional 12 MR cylindrical channels of 7.3 Å diameter.[71,72] Its structure is very similar to that of CIT-5 zeolite, and sorption properties of SSZ-24 should be similar to those of CIT-5 (see Table 1). The optimized structure of hexane sorbed on SSZ-24 zeolite with the loading of 1 hexane 48 SiO_2 units is shown in Figure 10. Hexane molecules being inclined with respect to the channel direction are located in the 12 MR channels, while the CH_3 groups at both ends of hexane molecule interacting with the zeolite walls. The heat of sorption obtained theoretically is 56.9 kJ/mol, which is near to the literature data obtained by chromatography (54.1 kJ/mol[14]) and gravimetry (68.4 kJ/mol[25]) as well as by theoretical calculations (54.0,[34] 67,[25] and ∼55−60 kJ/mol[65]).

Discussion

Effect of Ordering on the Heat of Sorption. On the basis of our calculations, different configurations of sorbed molecules can be found depending on the type of zeolite and loading. At low loadings, sorbed molecules can be located strictly in the center along the channel direction (as was observed for ZSM-22) or can be slightly moved from the center (as in the case of SSZ-24), slightly inclined (ZSM-12, SSZ-35), or even located

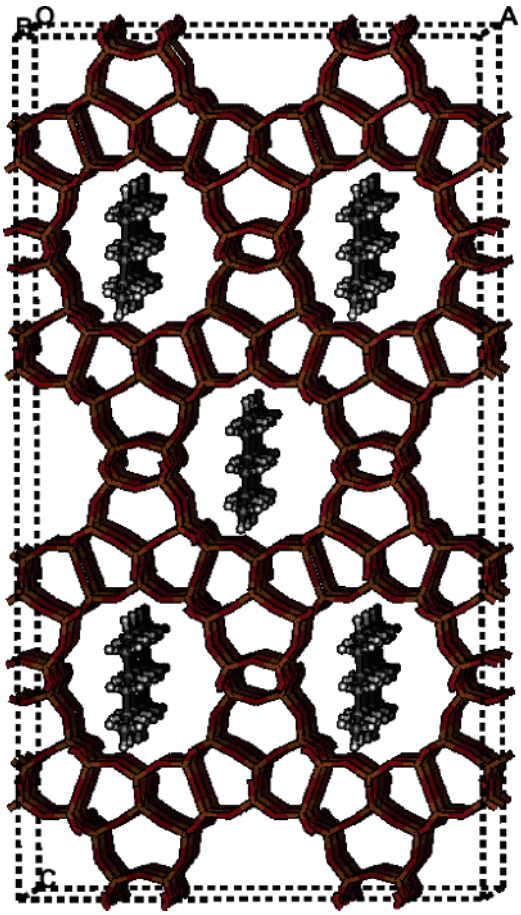

Figure 7. Optimized hexane molecules in CIT-5 zeolite. This corresponds to a loading of 1 hexane/16 SiO_2 units.

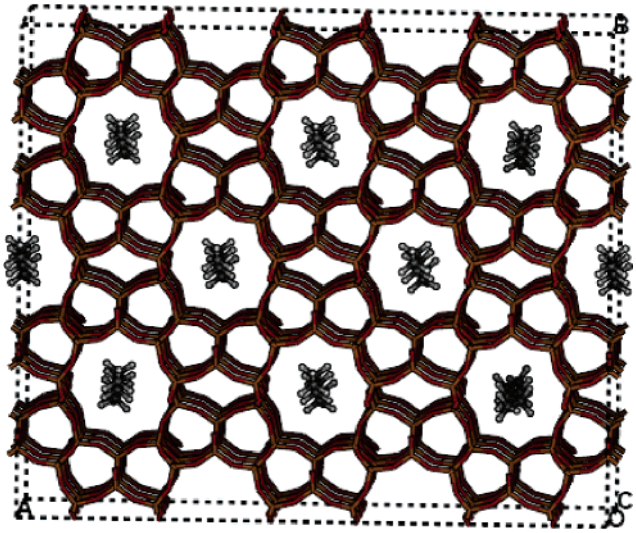

Figure 8. Optimized hexane molecules in ZSM-22 zeolite. This corresponds to a loading of 1 hexane/36 SiO_2 units.

perpendicularly (as for CIT-5). At high loadings the configuration of sorbed molecules changes optimizing the sorbate−sorbate and sorbate−zeolite interactions.

An increase of the enthalpy of sorption upon increasing the loading was observed for hydrocarbons on acidic and siliceous zeolites with different structure.[19,20,73,74] For example, an increase of 23 kJ/mol upon increasing the loading was reported for hexane on FAU zeolite.[20] This phenomenon can be explained by the increasing sorbate−sorbate interactions that are more pronounced for longer chains.[19,20,73,74] It should be taken into

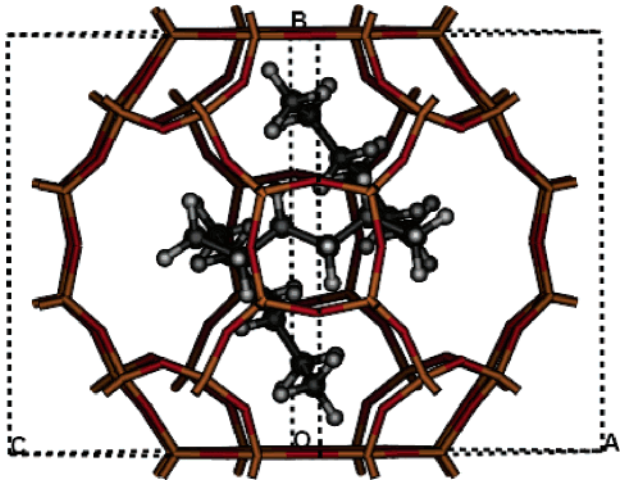

Figure 9. Optimized hexane molecules in zeolite-A. This corresponds to a loading of 1 hexane/8 SiO_2 units.

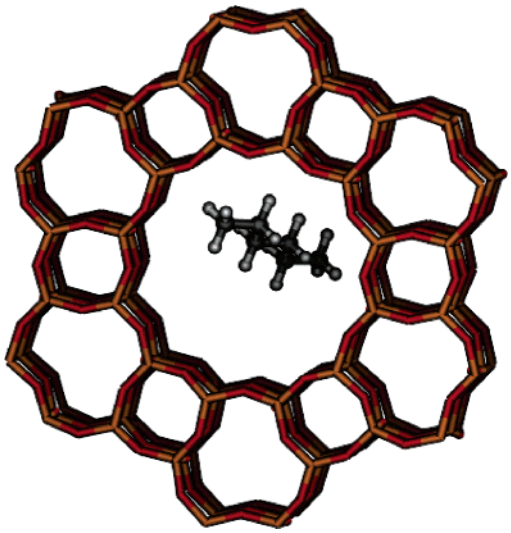

Figure 10. Optimized hexane molecules in SSZ-24 zeolite. This corresponds to low loading.

account that, besides sorbate−sorbate interaction, an entropic factor could also play an important role on the sorption properties, and logically, an increase in the loading should lead to a decrease of the entropy of molecules sorbed inside the channels.[32,75] The loss of entropy upon loading can be deduced from the configuration of molecules located inside channels (see Figures 3−10). At low coverage, hexane is sorbed close to the center of the pores with high translation and rotational freedom. On the other hand, at higher loading molecules are structured in different ways depending on the zeolite in order to optimize the interaction energies. In this case a complete loss of the levels of freedom occurs and the best fitting of molecules inside the pores can be observed. Because of such confinement, the adsorption energy increases by 6 kJ/mol for ZSM-12 zeolite (from 64.2 to 70.2 kJ/mol) and by 7.9 kJ/mol for SSZ-35 zeolite (from 54.4 to 62.3 kJ/mol). A similar situation was obtained for CIT-5 zeolite at high loadings; i.e., the molecules are structured inside the channels perpendicularly to their direction and parallel to each other (Figure 7).

A linear relationship between the entropy and energy of adsorption upon increasing the loading ("compensation effect") was reported for the linear paraffins on several zeolites.[22,76] From this point of view, a variation of adsorption entropy upon coverage leads to the same but opposite variation of enthalpy.[74]

This can explain the large range of values for heat of adsorption found in the literature for the same zeolite (see Table 1). For example, variations in adsorption energy from 33.1[34] to 53 kJ/mol[20] for FAU, from 54.0[34] to 68.4 kJ/mol[25] for AFI type, from 35.4[77] to 50 kJ/mol[25] for VFI aluminophosphates were found. If we accept the homogeneity of the surface energy of zeolites (since if zeolites would have heterogeneous energetic sites, sorption energy should decrease upon increasing the coverage), such variation of the heat of sorption will depend on the configuration of sorbed molecules inside the channels, which, in turn, depends on the loading. It should be noted that this conclusion is valid for zeolites, which have no or little preferential adsorption sites, where sorption occurs not as *surface coverage* but as *volume filling*, i.e., siliceous zeolites. For aluminum-containing zeolites the situation could be different, since preferential adsorption sites may exist.

In conclusion, we can say that in order to compare the effect of the pore dimension on the heat of sorption not only the diameter of the pore should be accounted but also the geometry of the sorbed molecule. The effect of entropy should increase the heat of adsorption to a maximum value, while the coverage reaches the saturation level, when the molecules are best fitted within the pores due to intermolecular repulsive interaction.

Effect of Pore Dimension from Literature Data and from This Work. Upon comparison of one-dimensional zeolites, linear relations can be observed between the pore dimension of aluminophosphates and the heat of sorption of hexane and small hydrocarbons.[25,78] Similar correlations can be obtained for methane, ethane, and propane molecules sorbed on FER, TON, MTW, and DON types of siliceous zeolites (heats of sorption of these molecules were taken from ref 26 and plotted against the average diameter of zeolite pores, not shown here). On zeolites with multidimensional structure, a nonlinear correlation was reported for C4−C10 *n*-paraffins.[8] The maximum heat was observed for zeolites with average pore diameter about 4−5 Å, as was mentioned before. At higher pore diameter the heat is decreasing.

In the case of mesoporous siliceous MCM-41 molecular sieves the sorption energy reaches the lowest value, but it is constantly higher than the heat of condensation, even with a pore size of about 100 Å. This phenomenon was ascribed to the "confinement effect", which is usually present in microporous systems.[36]

In Figure 11, we have plotted the heat of sorption of hexane on mono-dimensional ZSM-12, ZSM-22, SSZ-35, and CIT-5 as well as the tridimensional ITQ-29 pure silica zeolites vs the average pore diameter. The lowest sorption energy (39 kJ/mol) was found for ITQ-29 (LTA structure), which contains supercages of ∼11.4 Å diameter.[47] Because this heat is similar to that of hexane sorbed on amorphous silica gel (30 kJ/mol[68]) and on mesoporous silica MCM-41 (32−39 kJ/mol reported in ref 36), one can conclude that for pore diameters larger than 11 Å there is only little effect of confinement on the heat of sorption of *n*-hexane. Going to lower pore dimension zeolites, we observed the increase of the heat of sorption, which reaches a maximum at ∼83 kJ/mol for ZSM-22 zeolite (TON structure). Such a dependence is in agreement with the previous data published in the literature for zeolites with different pore diameters[19,25,79] (see Figure 12). It should be taken into account the large dispersion of results observed that could be due to (i) effect of loading, (ii) zeolite structural heterogeneity, which means that an average pore diameter cannot be strictly defined, and (iii) some differences due to the conditions of the experiments.

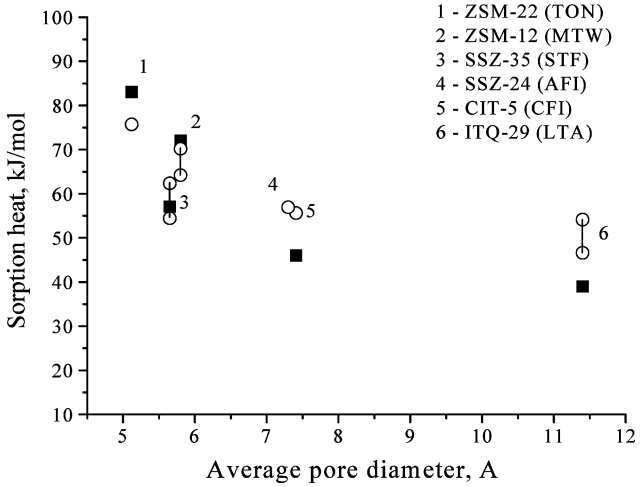

Figure 11. Dependence of the heat of hexane sorption on the average pore diameter of monodimensional siliceous zeolites (here included also ITQ-29). Squares correspond to data obtained experimentally by FTIR spectroscopy, and circles correspond to those obtained by calculations for high and low loadings. Numbers are related to different zeolites: 1, TON; 2, MTW; 3, STF; 4, AFI; 5, CFI; 6, ITQ-29.

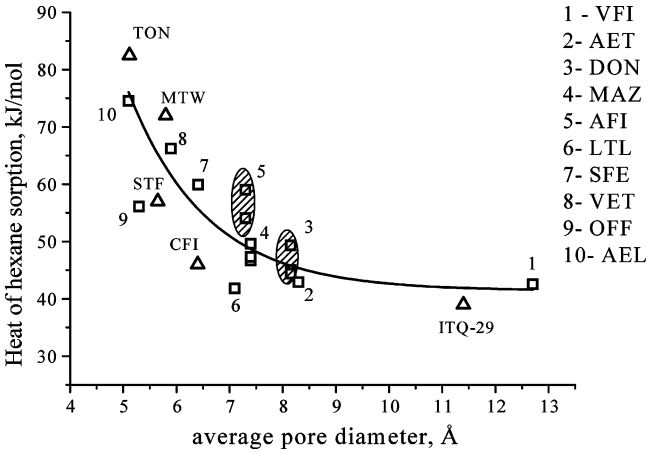

Figure 12. Literature (squares) and experimental (triangles) values of the heat of hexane sorption on monodimensional siliceous zeolites plotted vs average pore diameter of the zeolitic channels.

Conclusion

The sorption of hexane on pure silica monodimensional zeolites ZSM-12, ZSM-22, CIT-5, and SSZ-35 and on recently synthesized pure silica zeolite A (ITQ-29) was studied by FTIR spectroscopic and theoretical calculation methods. From the temperature dependence of the intensity of IR bands of sorbed hexane, the heats of sorption were determined and compared to the literature data. The decrease of the adsorption heat upon decreasing the pore diameter was obtained in agreement with the literature. Theoretical calculations clearly showed the accordance between the orientations of sorbed molecules, which are varied for different zeolites, and the heat of sorption of hexane. The increase of sorption heat at high loading could be attributed not only to the sorbate−sorbate and sorbate−zeolite interaction but also to the entropic effect. The maximum heat of sorption of hexane was clearly shown from the theoretical calculations to be achieved at conditions where the molecules are best fitted inside zeolite channels.

Acknowledgment. Dr. M. J. Diaz-Cabañas and Dr. S. Valencia are acknowledged for facilitating the zeolite samples. The authors thank Ministerio de Educación y Ciencia of Spain

for funding through projects MAT2003-07769-C02-01 and MAT2003-07945-C02-01.

References and Notes

(1) Mooiweer, H. H.; de Jong, K. P.; Kraushaar-Czarnetzki, B.; Stork, W. H. J.; Krutzen, B. C. H. *Stud. Surf. Sci. Catal.* **1996**, *84*, 2327.
(2) Houzvicka, J.; Ponec, V. *Catal. Rev.—Sci. Eng.* **1997**, *39*, 319.
(3) Corma, A. *J. Catal.* **2003**, *216*, 298.
(4) Haag, W. O. *Stud. Surf. Sci. Catal.* **1994**, *84*, 1375.
(5) Pieterse, J. A. Z.; Veefkind-Reyes, S.; Seshan, K.; Lercher, J. A. *J. Phys. Chem. B* **2000**, *104*, 5715.
(6) Savitz, S.; Siperstein, F.; Gorte, R. J.; Myers, A. L. *J. Phys. Chem. B* **1998**, *102*, 6865.
(7) Bárcia, P. S.; Silva, J. A. C.; Rodrigues, A. E. *Microporous Mesoporous Mater.* **2005**, *79*, 145.
(8) Bates, S. P.; van Well, W. J. M.; van Santen, R. A.; Smit, B. *J. Am. Chem. Soc.* **1996**, *118*, 6753.
(9) Bilgic, C.; Askin, A. *J. Chromatogr. A* **2003**, *1006*, 281.
(10) Chica, A.; Corma, A.; Miguel, P. J. *Catal. Today* **2001**, *65*, 101.
(11) Delgado, J. A.; Nijhuis, T. A.; Kapteijn, F.; Moulijn, J. A. *Chem. Eng. Sci.* **2004**, *59*, 2477.
(12) Denayer, J. F.; Baron, G. V.; Martens, J. A.; Jacobs, P. A. *J. Phys. Chem. B* **1998**, *102*, 3077.
(13) Denayer, J. F.; Bouyermaouen, A.; Baron, G. V. *Ind. Eng. Chem. Res.* **1998**, *37*, 3691.
(14) Denayer, J. F.; Ocakoglu, A. R.; Martens, J. A.; Baron, G. V. *J. Catal.* **2004**, *226*, 240.
(15) Denayer, J. F.; Souverijns, W.; Jacobs, P. A.; Martens, J. A.; Baron, G. V. *J. Phys. Chem. B* **1998**, *102*, 4588.
(16) Derouane, E. G.; Nagy, J. B.; Fernandez, C.; Gabelica, Z.; Laurent, E.; Maljean, P. *Appl. Catal.* **1988**, *40*, L1.
(17) Derouane, E. G.; Andre, J. M.; Lucas, A. A. *J. Catal.* **1988**, *110*, 58.
(18) Domokos, L.; Lefferts, L.; Seshan, K.; Lercher, A. *J. Catal.* **2001**, *203*, 351.
(19) Eder, F.; Lercher, J. A. *J. Phys. Chem. B* **1997**, *101*, 1273.
(20) Eder, F.; Lercher, J. A. *Zeolites* **1997**, *18*, 75.
(21) Eder, F.; Stockenhuber, M.; Lercher, J. A. In *Zeolites: A Refined Tool for Designing Catalytic Sites; Stud. Surf. Sci. Catal.*; Bonneviot, L., Kaliaguine, S., Eds.; Elsevier: Amsterdam, 1995; Vol. 97, p 495.
(22) Eder, F.; Stockenhuber, M.; Lercher, J. A. *J. Phys. Chem. B* **1997**, *101*, 5414.
(23) Fox, J. P.; Rooy, V.; Bates, S. P. *Microporous Mesoporous Mater.* **2004**, *69*, 9.
(24) Makowski, W.; Majda, D. *Thermochim. Acta* **2004**, *412*, 131.
(25) McCullen, S. B.; Reischman, P. T.; Olson, D. *Zeolites* **1993**, *13*, 640.
(26) Ndjaka, J.-M. B.; Zwanenburg, G.; Smit, B.; Schenk, M. *Microporous Mesoporous Mater.* **2004**, *68*, 37.
(27) Newalkar, B. L.; Jasra, R. V.; Kamath, V.; Bhat, S. G. T. *Adsorption* **1999**, *5*, 345.
(28) Olson, D. H.; Camblor, M. A.; Villaescusa, L. A.; Kuehl, G. H. *Microporous Mesoporous Mater.* **2004**, *67*, 27.
(29) Raybaud, P.; Patrigeon, A.; Toulhoat, H. *J. Catal.* **2001**, *197*, 98.
(30) Zhu, W.; Kapteijn, F.; Moulijn, J. A. *Phys. Chem. Chem. Phys.* **2000**, *2*, 1989.
(31) Arik, I. C.; Denayer, J. F.; Baron, G. *Microporous Mesoporous Mater.* **2003**, *60*, 111.
(32) Stach, H.; Fiedler, K.; Jänchen, J. *Pure Appl. Chem.* **1993**, *65*, 2193.
(33) Stach, H.; Lohse, U.; Thamm, H.; Schirmer, W. *Zeolites* **1986**, *6*, 74.
(34) Schenk, M.; Calero, S.; Maesen, T. L. M.; Vlugt, T. J. H.; van Benthem, L. L.; Verbeek, M. G.; Schnell, B.; Smit, B. *J. Catal.* **2003**, *214*, 88.
(35) Yoda, E.; Kondo, J. N.; Domen, K. *J. Phys. Chem. B* **2005**, *109*, 1464.
(36) Tanchoux, N.; Trens, P.; Maldonado, D.; Di renzo, F.; Fajula, F. *Colloids Surf., A* **2004**, *246*, 1.
(37) Smit, B. *Ind. Eng. Chem. Res.* **1995**, *34*, 4166.
(38) Maginn, E. J.; Bell, A. T.; Theodorou, D. N. In *Zeolites and Related Microporous Materials: State of the Art 1994*; *Stud. Surf. Sci. Catal.*; Weitkamp, J., Karge, H. G., Pfeifer, H., Hölderlich, W., Eds.; Elsevier: Amsterdam, 1994; Vol. 84, p 2099.
(39) Paukshtis, E. A.; Yurchenko, E. N. *Russ. Chem. Rev.* **1983**, *52*, 242.
(40) Meeks, O. R.; Rybolt, T. R. *J. Colloid Interface Sci.* **1997**, *196*, 103.
(41) Lee, C.; Parrillo, D. J.; Gorte, R. J.; Farneth, W. E. *J. Am. Chem. Soc.* **1996**, *118*, 3262.
(42) Silva, A. O. S.; Souza, M. J. B.; Aquino, J. M. F. B.; Fernandes Jr., V. J.; Araujo, A. S. *J. Therm. Anal. Calorim.* **2004**, *76*, 783.
(43) Zicovich-Wilson, C. M.; Corma, A.; Viruela, P. *J. Phys. Chem.* **1994**, *98*, 10863.
(44) Corma, A.; García, H.; Sastre, G.; Viruela, P. M. *J. Phys. Chem. B* **1997**, *101*, 4575.
(45) Barrer, R. M. *J. Colloid Interface Sci.* **1966**, *31*, 415.
(46) Jänchen, J.; Stach, H.; Uytterhoeven, L.; Mortier, W. J. *J. Phys. Chem.* **1996**, *100*, 12489.
(47) Corma, A.; Rey, F.; Rius, J.; Sabater, M. J.; Valencia, S. *Nature (London)* **2004**, *431*, 287.
(48) Wagner, P.; Zones, S. I.; Davis, M. E.; Medrud, R. C. *Angew. Chem., Int. Ed.* **1999**, *38*, 1269.
(49) Valyocsik, E. W. Synthesis of Zeolite ZSM-22, Canadian Patent 426820, 1986.
(50) Barret, P. A.; Diaz-Cabañas, M. J.; Camblor, M. A.; Jones, R. H. *J. Chem. Soc., Faraday Trans.* **1998**, *24*, 2475.
(51) Camblor, M. A.; Villaescusa, L. A.; Diaz-Cabanas, M. J. *Top. Catal.* **1999**, *9*, 59.
(52) Schuth, F.; Demuth, D.; Kallus, S. In *Zeolites and Related Microporous Materials: State of the Art 1994*; *Stud. Surf. Sci. Catal.*; Weitkamp, J., Karge, H. G., Pfeifer, H., Holderich, W., Eds.; Elsevier Science B.V.: Amsterdam, 1994; Vol. 84, p 1223.
(53) Roque-Malherbe, R. *Microporous Mesoporous Mater.* **2000**, *41*, 227.
(54) Richards, R. E.; Rees, L. V. C. *Langmuir* **1987**, *3*, 335.
(55) Du, H.; Kalyanaraman, M.; Camblor, M. A.; Olson, D. *Microporous Mesoporous Mater.* **2000**, *40*, 305−312.
(56) (a) Catlow, C. R. A.; Mackrodt, W. C. In *Computer Simulation of Solids*; Catlow, C. R. A., Mackrodt, W. C., Eds.; Springer: Berlin, 1982; Vol. 166, p 3. (b) Catlow, C. R. A.; Cormack, A. N. *Int. Rev. Phys. Chem.* **1987**, *6*, 227.
(57) (a) Gale, J. D. *J. Chem. Soc., Faraday Trans.* **1997**, *93*, 629. (b) Gale, J. D. *J. Phys. Chem. B* **1998**, *102*, 5423.
(58) Sanders, M. J.; Leslie, M.; Catlow, C. R. A. *J. Chem. Soc., Chem. Commun.* **1984**, 1271.
(59) Jackson, R. A.; Catlow, C. R. A. *Mol. Simul.* **1988**, *1*, 207.
(60) Kiselev, A. V.; Lopatkin, A. A.; Shulga, A. A. *Zeolites* **1985**, *5*, 261.
(61) Oie, T.; Maggiora, T. M.; Christoffersen, R. E.; Duchamp, D. J. *Int. J. Quantum Chem., Quantum Biol. Symp.* **1981**, *8*, 1.
(62) Ditchfield, R.; Hehre, W. J.; Pople, J. A. *J. Chem. Phys.* **1971**, *54*, 724.
(63) Harrison, R.; Nichols, J.; Straatsma, T.; Dupuis, M.; Bylaska, E.; Fann, G.; Windus, T.; Apra, E.; Anchell, J.; Bernholdt, D.; Borowski, P.; Clark, T.; Clerc, D.; Dachsel, H.; de Jong, B.; Deegan, M.; Dyall, K.; Elwood, D.; Fruchtl, H.; Glendenning, E.; Gutowski, M.; Hess, A.; Jaffe, J.; Johnson, B.; Ju, J.; Kendall, R.; Kobayash, R.; Kutteh, R.; Lin, Z.; Littlefield, R.; Long, X.; Meng, B.; Nieplocha, J.; Niu, S.; Rosing, M.; Sandrone, G.; Stave, M.; Taylor, H.; Thomas, G.; van Lenthe, J.; Wolinski, K.; Wong, A.; Zhang, Z. *NWChem, A Computational Chemistry Package for Parallel Computers*, 4.0th ed.; Pacific Northwest National Laboratory: Richland, WA, 2000.
(64) Dragoi, B.; Gervasini, A.; Dumitriu, E.; Auroux, A. *Thermochim. Acta* **2004**, *420*, 127.
(65) Guil, J. M.; Guil-López, R.; Perdigón-Melón, J. A.; Corma, A. *Microporous Mesoporous Mater.* **1998**, *22*, 269.
(66) Martinez-Triguero, J.; Diaz-Cabañas, M. J.; Camblor, M. A.; Fornes, V.; Maesen, T. L. M.; Corma, A. *J. Catal.* **1999**, *182*, 463.
(67) de Gauw, F. J. M. M.; van Grondelle, J.; van Santen, R. A. *J. Catal.* **2002**, *206*, 295.
(68) Roshchina, T. M.; Shonia, N. K.; Kazmina, A. A.; Gurevich, K. B.; Fadeev, A. Y. *J. Chromatogr. A* **2001**, *931*, 119.
(69) Tumsek, F.; Inel, O. *Chem. Eng. J.* **2003**, *94*, 57.
(70) Auerbach, S. M.; Joussez, F.; Vercauteren, D. P. In *Computer Modelling of Microporous Mesoporous Materials*; Catlow, C. R. A., van Santen, R. A., Smit, B., Eds.; Elsevier: Amsterdam, 2004; p 49.
(71) Baerlocher, C.; Meier, W. M.; Olson, D. *Atlas of Zeolite Structure Types*, 5th revised ed.; Elsevier: Amsterdam, 2001.
(72) Bailek, R.; Meier, W. M.; Davis, M. E.; Annen, M. J. *Zeolites* **1991**, *11*, 438.
(73) Thamm, H.; Stach, H.; Fiebig, W. *Zeolites* **1983**, *3*, 95.
(74) Thamm, H. *Zeolites* **1987**, *7*, 341.
(75) Myers, A. L. *Colloids Surf., A* **2004**, *241*, 9.
(76) Ruthven, D. M.; Kaul, B. K. *Adsorption* **1998**, *4*, 269.
(77) Liu, J. X.; Dong, M.; Qin, Z. F.; Wang, J. G. *J. Mol. Struct. (THEOCHEM)* **2004**, *679*, 95.
(78) Jänchen, J.; Stach, H.; Grobet, P. J.; Martens, J. A.; Jacobs, P. A. *Zeolites* **1992**, *12*, 9.
(79) Ocakoglu, R. A.; Denayer, J. F. M.; Marin, G. B.; Martens, J. A.; Baron, G. V. *J. Phys. Chem. B* **2003**, *107*, 398.
(80) Maesen, T. L. M.; Schenk, M.; Vlugt, T. J. H.; de Jonge, J. P.; Smit, B. *J. Catal.* **1999**, *188*, 403.
(81) Díaz, E.; Ordóñez, S.; Vega, A.; Coca, J. *J. Chromatogr. A* **2004**, *1049*, 139.

(82) Silva, J. A. C.; Rodrigues, A. E. *AIChE J.* **2004**, *43*, 2524.
(83) Vlugt, T. J. H.; Krishna, R.; Smit, B. *J. Phys. Chem. B* **1999**, *103*, 1102.
(84) Dubbeldam, D.; Calero, S.; Vlugt, T. J. H.; Krishna, R.; Maesen, T. L. M.; Smit, B. *J. Phys. Chem. B* **2004**, *108*, 12301.
(85) Du, H.; Kalyanaraman, M.; Camblor, M. A.; Olson, D. *Microporous Mesoporous Mater.* **2000**, *40*, 305.
(86) Eder, F.; He, Y.; Nivarthy, G.; Lercher, J. A. *Pays-Bas* **1996**, *115*, 531.
(87) Corma, A.; Chica, A.; Guil, J. M.; Llopis, F. J.; Mabilon, G.; Perdigón-Melón, J. A.; Valencia, S. *J. Catal.* **2000**, *189*, 382.
(88) Qiao, S. Z.; Bhatia, S. K.; Nicholson, D. *Langmuir* **2004**, *20*, 389.
(89) Prè, P.; Delage, F.; Faur-Brasquet, C.; Le Cloirec, P. *Fuel Process. Technol.* **2002**, *77*−*78*, 345.
(90) Montes-Morán, M. A.; Paredes, J. I.; Martínez-Alonso, A.; Tascón, J. M. D. *J. Colloid Interface Sci.* **2002**, *247*, 290.
(91) Castello, G.; D'Amato, G. *J. Chromatogr.* **1975**, *107*, 1.